




Accuracy of discrete- and continuous-time mean-field theories for epidemic processes on complex networks

Diogo H. Silva ¹, Francisco A. Rodrigues ¹, and Silvio C. Ferreira ^{2,3}

¹*Instituto de Ciências Matemáticas e de Computação, Universidade de São Paulo, São Carlos, SP 13566-590, Brazil*

²*Departamento de Física, Universidade Federal de Viçosa, 36570-900 Viçosa, Minas Gerais, Brazil*

³*National Institute of Science and Technology for Complex Systems, 22290-180, Rio de Janeiro, Brazil*



(Received 15 February 2024; accepted 27 June 2024; published 17 July 2024)

Discrete- and continuous-time approaches are frequently used to model the role of heterogeneity on dynamical interacting agents on the top of complex networks. While, on the one hand, one does not expect drastic differences between these approaches, and the choice is usually based on one's expertise or methodological convenience, on the other hand, a detailed analysis of the differences is necessary to guide the proper choice of one or another approach. We tackle this problem by investigating both discrete- and continuous-time mean-field theories for the susceptible-infected-susceptible (SIS) epidemic model on random networks with power-law degree distributions. We compare the discrete epidemic link equations (ELE) and continuous pair quenched mean-field (PQMF) theories with the corresponding stochastic simulations, both theories that reckon pairwise interactions explicitly. We show that ELE converges to the PQMF theory when the time step goes to zero. We performed an epidemic localization analysis considering the inverse participation ratio (IPR). Both theories present the same localization dependence on network degree exponent γ : for $\gamma < 5/2$ the epidemics are localized on the maximum k -core of networks with a vanishing IPR in the infinite-size limit while, for $\gamma > 5/2$, the localization happens on hubs that do not form a densely connected set and leads to a finite value of the IPR. However, the IPR and epidemic threshold of ELE depend on the time-step discretization such that a larger time step leads to more localized epidemics. A remarkable difference between discrete- and continuous-time approaches is revealed in the epidemic prevalence near the epidemic threshold, in which the discrete-time stochastic simulations indicate a mean-field critical exponent $\theta = 1$ instead of the value $\theta = 1/(3 - \gamma)$ obtained rigorously and verified numerically for the continuous-time SIS on the same networks.

DOI: [10.1103/PhysRevE.110.014302](https://doi.org/10.1103/PhysRevE.110.014302)

I. INTRODUCTION

The broad diversity of spreading processes [1,2] and the role that they have assumed in our contemporary society call for the development of theoretical tools [3] to predict outbreaks and ways to mitigate their consequences [4]. For example, the recent epidemic outbreaks of Zika virus [5], Ebola [6], and COVID-19 pandemics [7,8] enhanced the development of compartmental models [1,9] for epidemic processes on populations.

The heterogeneity of contacts among individuals influences the spreading process [1,2] and these connection patterns can be tackled using complex networks theory [10,11]. Theoretical frameworks for epidemic models running on the top of complex networks allow one to investigate the coupling between the dynamic and structural features of the system. In continuous-time approaches, different mean-field theories are widely applied to address these features. The whole network structure is considered in the quenched mean-field (QMF) [2,3] theory that neglects dynamical correlations of the epidemic states of connected vertices. This theory is improved by considering correlations in a pairwise level in the pair quenched mean-field (PQMF) [12,13] theory. These theories have been applied to investigate the limit of low epidemic prevalence (average fraction of infected nodes) [12–16], while

the PQMF theory also presents an excellent concordance with stochastic simulations in the regime of high prevalence [17].

Some aspects of actual epidemic processes, such as the daily update of reported cases by surveillance systems [4] and computational facilities [7,18–22], lead to the wide use of discrete-time versions of epidemic dynamics. Note that a straightforward discretization of continuous-time theoretical approaches presents limitations [20] as, for example, the epidemic prevalence in the supercritical regime converging to nontrivial fixed points [23]—the more striking for longer time steps [24]. Pitfalls of the discrete-time framework can be fixed using the nonlinear dynamical system (NDLS) approach [25,26], which explores the representation of the dynamics as Markov chains. This approach was generalized in the so-called microscopic Markov-chain approach (MMCA) [19], which was adapted and applied to different problems, such as propagation of information and epidemics on multiplex networks [21,27,28] and metapopulation [29,30] modeling of spatiotemporal epidemic spreading [7,31]. In particular, a discrete-time counterpart of the PQMF theory [12], adding dynamical correlations to the MMCA, called epidemic linking equations (ELE) [22], was applied to investigate optimal immunization strategies in complex networks.

Epidemic or, more generally, dynamical processes on networks are featured by localization phenomena where the

activity can be highly concentrated on a finite [16,32] or subextensive [32,33] part of the network. Localization in epidemic processes was formerly associated with the leading eigenvector of the adjacency matrix that rules the local epidemic prevalence of the QMF theory [16]. The idea was extended to PQMF [13] and, later, to generic epidemic processes on networks [32], including stochastic simulations. The accuracy of mean-field approaches is correlated with the level of localization of the activity near the epidemic threshold in each theory [13,34]. The more localized the outcome of a mean-field theory, the less accurate its prediction of the epidemic threshold [13].

Two types of localization have been associated with the SIS epidemic activation on random power-law networks depending on the degree exponent γ [1]. One is related to the activation of isolated and another to a set of densely connected hubs of networks given by the maximum k -core decomposition [32,33,35,36]. In the former case, nodes of degree $K \sim k_{\max}$ and their nearest neighbors are activated at a threshold $\lambda_c \sim 1/\sqrt{k_{\max}}$, which corresponds to a star graph epidemic threshold [12], while in the latter the activation happens on a densely connected core of size N_{core} at the threshold $\lambda_c \sim 1/N_{\text{core}}$, which corresponds to complete graph threshold. Since $N_{\text{core}} \sim \langle k^2 \rangle / \langle k \rangle \sim k_{\max}^{3-\gamma}$ for uncorrelated networks [16,37], one has that the hub activation rules the threshold when $k_{\max}^{3-\gamma} \ll \sqrt{k_{\max}}$, which means $\gamma > 5/2$.

In this paper, we develop a numerical study of the accuracy of discrete-time theoretical approaches represented by MMCA and ELE in comparison with synchronous-update stochastic simulations. We focus on determining the epidemic threshold and prevalence of the susceptible-infected-susceptible model (SIS) [1] in uncorrelated networks with power-law degree distributions, where an infected individual heals spontaneously with rate μ and transmits the disease to its susceptible neighbors with rate β (continuous-time version) per contact. This simple model presents far from trivial features. For example, the epidemic threshold is null in the thermodynamic limit, where the system size goes to infinity, in the case of power-law degree distribution regardless of the degree exponent γ [38,39]. In the discrete-time SIS model, the healing and infection probabilities are given by $g = \mu \Delta t$ and $r = \beta \Delta t$, respectively. When these probabilities assume large values, the discrete-time SIS deviates substantially from its continuous-time version [40]. Indeed, in the limit of high infection probability and prevalence, Chang and Cai [41] claimed that there is no linear mapping from discrete- to continuous-time dynamics, while Zhang *et al.* [42] proposed a nonlinear relation between rates and probabilities to circumvent this drawback.

Different theoretical approaches are compared with either optimized Gillespie (OGA) [43] or synchronous update (SUA) [40] algorithms for continuous- and discrete-time simulations, respectively. We report that, as in the continuous-time limit [12,13,17], the introduction of dynamical correlation in ELE improves the accuracy of the MMCA approach in describing the epidemic threshold and epidemic prevalence obtained in SUA. We also performed an epidemic localization analysis [32] and a nonperturbative (high prevalence regime) numerical integration, showing that ELE presents the same characteristics of the continuous-time limit obtained with

PQMF theory [13]: localization on the maximum k -core [36] for $\gamma < 5/2$ and on a finite set of nodes (hubs) for $\gamma > 5/2$ near to the epidemic threshold (low-prevalence regime) concomitant with a very good accuracy in the high-prevalence regime. Finally, discrete-time (no small time steps) stochastic simulations are consistent with a mean-field critical exponent $\theta = 1$ associated to vanishing of the epidemic threshold near to the epidemic threshold instead of the value $\theta = 1/(3 - \gamma)$ obtained rigorously [39] and verified numerically [13] in the continuous-time simulations of the SIS model on the same set of power-law networks.

The remainder of this paper is organized as follows. In Sec. II, we present the continuous- and discrete-time theories and demonstrate that ELE (MMCA) converges to PQMF (QMF) in the limit $\Delta t \rightarrow 0$. Section III starts with a discussion about the accuracy of continuous and discrete theories in predicting the epidemic threshold. This analysis is extended to localization and epidemic prevalence. Finally, in Sec. IV, we draw our conclusions and prospects.

II. ANALYTICAL AND SIMULATION APPROACHES

A. Continuous-time mean-field theories

In the QMF theory, the whole network structure is considered by the introduction of the adjacency matrix, defined as $A_{ij} = 1$ if nodes i and j are connected and $A_{ij} = 0$ otherwise, while dynamical correlations are neglected assuming that the probability ρ_i that a node i is infected does not depend on the states of its contacts. Thus the dynamical equation for evolution of ρ_i is [1–3]

$$\frac{d\rho_i}{dt} = -\mu\rho_i + \beta(1 - \rho_i) \sum_{i=1}^N A_{ij}\rho_j, \quad (1)$$

where the first term on the right-hand side corresponds to spontaneous healing, while the second one is the infection. If dynamical correlations are taken into account in a pair level in the named PQMF theory [12,13], the dynamical equation becomes

$$\frac{d\rho_i}{dt} = -\mu\rho_i + \beta \sum_{i=1} A_{ij}\phi_{ij}, \quad (2)$$

in which $\phi_{ij} = [S_i, I_j]$ is the probability that nodes i and j are in the states susceptible and infected, respectively. Note that $\phi_{ij} \approx (1 - \rho_i)\rho_j$ leads to the QMF theory, Eq. (1). Following Ref. [12], the evolution of ϕ_{ij} is given by

$$\begin{aligned} \frac{d\phi_{ij}}{dt} = & - (2\mu + \beta)\phi_{ij} + \mu\rho_j + \beta \sum_{l=1} \frac{\omega_{ij}\phi_{jl}}{(1 - \rho_j)} (A_{jl} - \delta_{il}) \\ & - \beta \sum_{l=1} \frac{\phi_{ij}\phi_{il}}{(1 - \rho_i)} (A_{il} - \delta_{lj}), \end{aligned} \quad (3)$$

in which $\omega_{ij} = [S_i, S_j] = 1 - \rho_i - \phi_{ij}$. Close enough to the epidemic threshold, the QMF and PQMF theories can be described by the spectral properties of the adjacency matrix in the former [14,16] and a weighted adjacency matrix in the latter [13].

B. Discrete-time mean-field theories

The general form for the temporal evolution of the probability that a node i is infected, i.e., ρ_i , in the MMCA [19] assumes the form

$$\rho_i(t + \Delta t) = (1 - \mu \Delta t) \rho_i(t) + [1 - q_i(t)][1 - \rho_i(t)] + \mu \Delta t [1 - q_i(t)] \rho_i(t), \quad (4)$$

in which $q_i(t)$ is the probability that node i was not infected in the corresponding time step

$$q_i(t) = \prod_{j=1}^N [1 - \beta \Delta t A_{ij} \rho_j(t)]. \quad (5)$$

In Eq. (4), the first term stands for the probability that node i remains infected, while in the second term is the probability that a susceptible node i is infected by any of its contacts. Finally, the last term reckons the probability that an infected node recovers and is reinfected by one of its neighbors during the time step Δt . We compare both MMCA and ELE with the same synchronous discrete-time simulations (see Sec. II C). So, the MMCA equation investigated is [44]

$$\rho_i(t + \Delta t) = (1 - \mu \Delta t) \rho_i(t) + [1 - q_i(t)][1 - \rho_i(t)]. \quad (6)$$

Note that an oscillating (period 2) epidemic prevalence is observed in both MMCA [44] and ELE [22] theories without reinfections and the steady-state prevalence is calculated as the arithmetic average of the values.

In the pairwise ELE approach [22], the system is described in terms of the joint probabilities $\phi_{ij} = [S_i, I_j]$, $\omega_{ij} = [S_i, S_j]$, and $\psi_{ij} = [I_i, I_j]$ given the states of connected pairs of nodes i and j . In particular, the evolution of ϕ_{ij} is derived in Ref. [22] and given by

$$\phi_{ij}(t + \Delta t) = \omega_{ij}(t) q_{ij}(t) [1 - q_{ji}(t)] + \mu \Delta t (1 - \mu \Delta t) \psi_{ij}(t) + \mu \Delta t [1 - (1 - \beta \Delta t) q_{ji}(t)] \phi_{ji}(t) + (1 - \mu \Delta t) (1 - \beta \Delta t) q_{ij}(t) \phi_{ij}(t), \quad (7)$$

where

$$q_{ij}(t) = \prod_{l=1, l \neq j}^N \left(1 - \beta \Delta t A_{li} \frac{\phi_{il}(t)}{1 - \rho_i(t)} \right) \quad (8)$$

$$\frac{\phi_{ij}(t + \Delta t) - \phi_{ij}(t)}{\Delta t} = \mu \psi_{ij}(t) - (\beta + \mu) \phi_{ij}(t) + \beta \sum_{l=1}^N \frac{\omega_{ij}(t) \phi_{lr}(t)}{1 - \rho_j(t)} (A_{rj} - \delta_{ri}) - \beta \sum_{l=1}^N \frac{\phi_{ij}(t) \phi_{lr}(t)}{1 - \rho_i(t)} (A_{ri} - \delta_{rj}) + O(\beta \Delta t). \quad (13)$$

Finally, considering the relations $\rho_j = \psi_{ij} + \phi_{ij}$ and $1 - \rho_i = \omega_{ij} + \phi_{ij}$, in the limit of $\Delta t \rightarrow 0$, Eqs. (12) and (13) converge to Eqs. (2) and (3).

C. Stochastic simulations

QMF and PQMF approaches are compared with continuous-time stochastic simulations implemented using the optimized Gillespie algorithm (OGA) [43]. In this algorithm, the probabilities of healing and infection are determined by the number of infected nodes N_{inf} and the total

is the probability that a susceptible node i is not infected by any of its neighbors (excluding node j) in the step t . Similar equations can be built for other joint probabilities; see Ref. [22]. The epidemic prevalence in the whole system is expressed as [22]

$$\rho = \frac{1}{N} \sum_{i=1}^N \frac{1}{k_i} \sum_{j=1}^N A_{ji} (\phi_{ji} + \omega_{ij}), \quad (9)$$

where k_i is the degree of node i .

The effects of dynamical correlations in ELE theory become clearer for the variable $\rho_i = \psi_{ij} + \phi_{ij}$ that evolves as

$$\rho_i(t + \Delta t) = (1 - \mu \Delta t) \rho_i(t) + [1 - q_{ij}(t)][1 - \rho_i(t)] + \beta \Delta t q_{ij}(t) \phi_{ij}(t). \quad (10)$$

The first and second terms have the similar form and interpretation of Eq. (4). The last term stands for the probability that nodes i and j are susceptible and infected, respectively, and node i is infected by node j .

The continuous- and discrete-time mean-field theories are equivalent in the regime of $\Delta t \rightarrow 0$. We now show the equivalence between ELE and PQMF, while one can easily demonstrate the equivalence between MMCA and QMF following similar steps. To leading order in Δt , Eq. (8) becomes

$$q_{ij}(t) = 1 - \beta \Delta t \sum_{r=1}^N \frac{\phi_{ir}(t)}{1 - \rho_i(t)} (A_{ri} - \delta_{rj}) + O(\beta \Delta t), \quad (11)$$

where $O(x)$ represent terms negligible if compared with x . Substituting Eq. (11) in Eqs. (7) and (10) leads to

$$\frac{\rho_i(t + \Delta t) - \rho_i(t)}{\Delta t} = -\mu \rho_i(t) + \beta \sum_r A_{ri} \phi_{ir} + O(\beta \Delta t) \quad (12)$$

and

number of edges emanating from them N_{SI} . In each time step, with probability

$$q = \frac{\mu N_{\text{inf}}}{\mu N_{\text{inf}} + \beta N_{\text{SI}}}, \quad (14)$$

an infected node is chosen at random and healed. With probability $1 - q$ an infected node i is chosen with probability proportional to its degree k_i . If the randomly chosen neighbor j is susceptible, it becomes infected; otherwise, no change of

state is implemented. The time is incremented by

$$\delta t = \frac{-\ln u}{\mu N_{\text{inf}} + \beta N_{\text{SI}}}, \quad (15)$$

where u is a pseudorandom number uniformly distributed in the interval $(0,1)$.

The discrete-time simulations are performed using the synchronous updating algorithm (SUA) [40,41,45], in which all nodes of the network have their states simultaneously updated in a discrete time step, Δt . For the SIS dynamics, each susceptible node becomes infected with probability $1 - (1 - \beta \Delta t)^{n_{\text{inf}}}$, in which n_{inf} is the number of infected contacts while an infected node becomes susceptible with probability $\mu \Delta t$. Finally, the time is incremented by Δt .

In both, continuous and discrete simulations, when the system falls into the absorbing state, the dynamics returns to a previously visited active configuration using the standard quasistationary (QS) method [46,47]. In this method, a list of M configurations is built and constantly updated by replacing a randomly chosen configuration by the current one with a probability P_{rep} per unit of time. In both cases, we adopted $M = 50$ and $P_{\text{rep}} = 0.01$. The QS averages were performed considering the averaging time varying from $t_{\text{av}} = 10^5$ to 10^6 time units after a relaxation time $t_{\text{rx}} = 10^5$ time units, the longer averaging times for the lower densities where fluctuations are more relevant. To compare the mean-field theories with QS simulations, we estimate the epidemic threshold using the peak of dynamical susceptibility defined as $\chi = N(\langle \rho^2 \rangle - \langle \rho \rangle^2) / \langle \rho \rangle$ [48].

III. RESULTS

We investigate both mean-field theories and stochastic simulations on synthetic networks with power-law degree distributions for different degree exponents generated by the uncorrelated configuration model (UCM) [49]. This model has upper cutoff $k_c \lesssim \sqrt{N}$ that guarantees the absence of degree correlations for very large networks. In principle, dynamics very localized around hubs can produce multiple peaks in $\chi(\lambda)$ curves [48]. Here, we used networks with cutoffs in the degree distribution that avoid the multiplicity of peaks; see Ref. [13] for more details.

A. Epidemic threshold

The MMCA and QMF predict the same epidemic threshold for the SIS dynamics, given by [1,19]

$$\lambda_c = \frac{\beta}{\mu} = \frac{1}{\Lambda_1} \quad (16)$$

in which Λ_1 is the largest eigenvalue of the adjacency matrix. The epidemic threshold of the ELE approach is given by [22]

$$\lambda_c = \frac{\beta}{\mu} = \frac{1}{\Omega_1}, \quad (17)$$

where Ω_1 is the largest eigenvalue of the matrix B_{ij} given by

$$B_{ij} = (1 - \Upsilon)A_{ij} - \Upsilon k_i \delta_{ij} \quad (18)$$

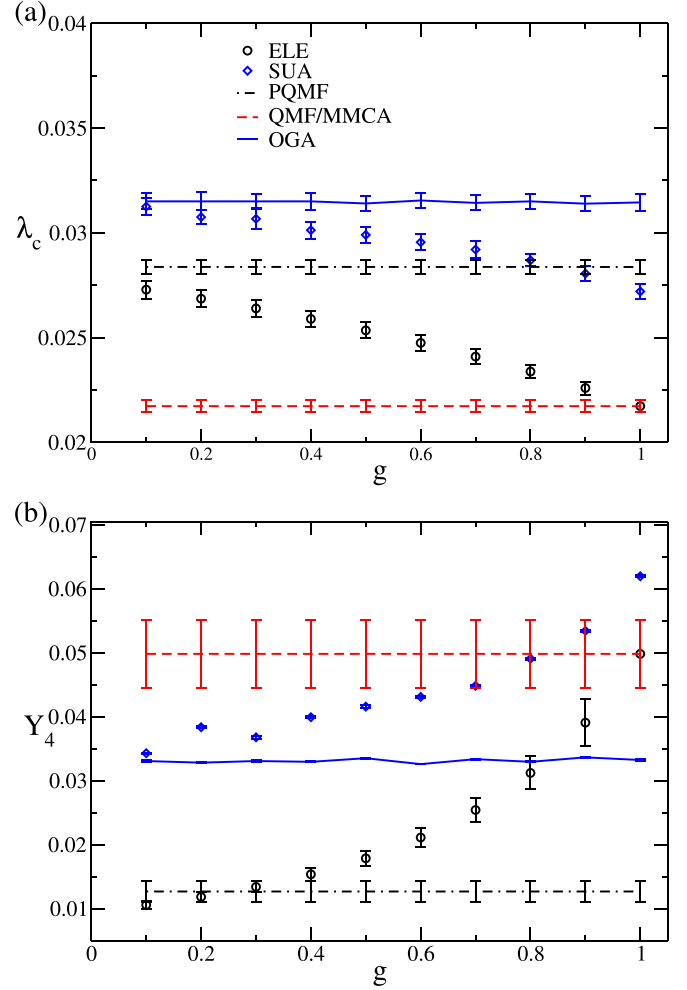


FIG. 1. Comparison of stochastic simulations and mean-field theories for SIS dynamics on uncorrelated PL networks with $\gamma = 2.8$, $N = 10^6$, and $k_c = 2\sqrt{N}$. (a) Epidemic threshold and (b) IPR are shown as functions of $g = \mu \Delta t$ with $\mu = 1$. Symbols and lines represent discrete- and continuous-time versions of stochastic simulations and theoretical frameworks, respectively. In (b), the IPR of both OGA and SUA stochastic simulations correspond to NAV multiplied by 10, for the sake of visibility. Averages were computed over 10 network-independent realizations.

in which δ_{ij} is the Kronecker delta symbol and

$$\Upsilon = \frac{\beta(1-g)}{\mu(2-g) + 2\beta(1-g)}. \quad (19)$$

For the PQMF theory, the epidemic threshold is obtained when the largest eigenvalue of the matrix [12]

$$L_{ij} = -\left(\mu + \frac{\beta^2 k_i}{2\mu + 2\beta}\right)\delta_{ij} + \frac{\beta(2\mu + \beta)}{2\mu + 2\beta}A_{ij} \quad (20)$$

is null. When $g = \mu \Delta t \rightarrow 0$ we have $\Upsilon = \beta/(\mu + 2\beta)$ and

$$L_{ij} = \mu \delta_{ij} - \beta B_{ij}, \quad (21)$$

where we confirm that the epidemic threshold of ELE converges to the PQMF theory. Moreover, for $g \rightarrow 1$ we have that $B_{ij} \rightarrow A_{ij}$ and ELE threshold goes to the same value of the QMF theory. Figure 1(a) presents the ELE and MMCA

epidemic thresholds as functions of g for fixed $\mu = 1$ as well as the results of PQMF theory with $\mu = 1$, where one can see the ELE's threshold decreases monotonically from the PQMF to the QMF theory result as g increases from 0 to 1. Figure 1(a) compares simulations and mean-field theories on a power-law network with $\gamma = 2.8$, $N = 10^6$ nodes, and $k_c = 2\sqrt{N}$. Discrete- and continuous-time simulations depart from each other as the time increment increases. The discrete case threshold decays with $g = \mu\Delta t$, showing a dependence on the method as already discussed in Ref. [40]. Observe that ELE reproduces qualitatively the decays of the threshold observed on discrete-time stochastic simulations (SUA), which does not happen with MMCA that provides a constant threshold. The ELE approximation deviates more from the discrete-time simulations as the time step increases; the highest precision happens in the limit $g \ll 1$ when it converges to the PQMF theory. These results hold for other values of γ (data not shown), presenting a greater accuracy when $\gamma < 2.5$.

B. Localization

To determine the localization pattern of both simulations and mean-field theories, we use the normalized activity vector (NAV) defined as [32]

$$\varphi_i = \frac{\rho_i}{\sqrt{\sum_{j=1}^N \rho_j}}, \quad (22)$$

where the local prevalence $\{\rho_i\}$ is computed at the epidemic threshold for different approaches (continuous, discrete, mean field, and simulations). The localization of the NAV is quantified using the inverse partition ratio (IPR) [16] defined as

$$Y_4(\varphi) = \sum_{i=1}^N \varphi_i^4. \quad (23)$$

The IPR converges to a finite value in the infinite-size limit if the localization happens on a finite set of nodes and scales as $Y_4 \sim N^{-1}$ for a delocalized state involving an extensive component of the network [16]. For MMCA [19] and QMF mean-field [16] approaches the local prevalence at the epidemic threshold is asymptotically proportional to the principal eigenvector (PVE), corresponding to the largest eigenvalue of the adjacency matrix. In the PQMF theory, the epidemic prevalence is proportional to the PVE of the Jacobian matrix L_{ij} , Eq. (20), evaluated at $\lambda = \lambda_c$ as shown in Ref. [13]. These relations are easily obtained within each theoretical approach as illustrated for ELE in the sequence of the paper.

Very close to the epidemic threshold, the local prevalence is given by [see Eq. (17) of Ref. [22]]

$$\rho_i = \frac{\beta}{\mu} \sum_j B_{ij} \rho_j. \quad (24)$$

Let $\Omega_1 \geq \Omega_2 \geq \dots, \Omega_N$ be the eigenvalues corresponding to the eigenvectors $\mathbf{b}^{(1)}, \mathbf{b}^{(2)}, \dots, \mathbf{b}^{(N)}$ of B_{ij} . Expanding $\rho_j =$

$\sum_l c^{(l)} b_j^{(l)}$ in the basis $\{\mathbf{b}^{(l)}\}$, one obtains

$$\begin{aligned} \rho_i &= \frac{\beta}{\mu} \sum_l c^{(l)} \sum_j B_{ij} b_j^{(l)} = \frac{\beta}{\mu} \sum_l \Omega_l c^{(l)} b_i^{(l)}, \\ \rho_i &\approx \frac{\beta}{\mu} \Omega_1 b_i^{(1)} \left[1 + \mathcal{O}\left(\frac{\Omega_2}{\Omega_1}\right) \right]. \end{aligned} \quad (25)$$

If B_{ij} has a spectral gap $\Omega_1 \gg \Omega_2$, that is usually the case investigated in the present paper, we find $\rho_i \sim b_i^{(1)}$. For simulations, we consider the QS local prevalence evaluated at the epidemic threshold [32]. Figure 1(b) shows the IPR as a function of g for different approaches. Corresponding values for the continuous-time are shown for the sake of comparison. While MMCA has a localization that does not depend on the time-step size, the epidemics become more localized as the time step increases for both ELE and SUA simulations, being minimal when $g \rightarrow 0$ and maximal when $g \rightarrow 1$. Note that the PVE of B_{ij} converges to that of L_{ij} when $g \rightarrow 0$ and to that of A_{ij} when $g \rightarrow 1$; see Eq. (18). Therefore, we have seen that discrete approaches, both simulation and ELE, present stronger localization when compared with their continuous-time counterparts.

A detailed finite-size analysis of the epidemic threshold and localization in ELE and discrete-time simulations are presented in Fig. 2. For $\gamma = 2.3$ shown Figs. 2(a) and 2(d), we have an agreement between simulations and theory and an independence with the time-step size. This behavior is indeed expected for $\gamma = 2.3$ since the ELE epidemic threshold and PVE interpolate between QMF and PQMF theories as g varies in the range (0,1), while the continuous-time mean-field theories match each other for $\gamma < 5/2$ [12,13]. The IPR is consistent with a subextensive localization characterized by sublinear scaling $Y_4 \sim N^{-(3-\gamma)/2}$ that depicts an activity localized in the maximum k -core [32,35], which is a densely connected subgraph accessed by a k -core decomposition [37]. For $\gamma > 5/2$, however, the localization increases with size in ELE and saturates for stochastic simulations. Concomitantly, we observed a worse performance of ELE to predict the epidemic threshold as the network size increases, with the worse for larger γ where localization is stronger, as previously reported for PQMF theory [13]. We also see that the finite time steps raise the localization effects, reducing ELE accuracy as also shown in Fig. 1. This aspect should be taken into account in the choice of the theoretical approach to model the epidemics.

C. Epidemic prevalence

We analyzed the epidemic prevalence for both discrete-time simulations and ELE mean-field theory. The infection rate was scaled according to the ELE prediction $\rho \sim \lambda\Omega_1 - 1$. To analyze the critical exponent θ , defined by $\rho \sim (\lambda - \lambda_c)^\theta$, of the discrete-time SIS dynamics and ELE, we consider the case in which $\gamma < 2.5$, where the theory presents a great accuracy in predicting the epidemic threshold. We analyze the region in which $\lambda\Omega_1^{\text{ELE}} - 1 \leq 1$ and observed an almost perfect agreement between ELE and simulations, in which $\rho \sim (\lambda\Omega_1^{\text{ELE}} - 1)^\theta$ with $\theta = 1$, if λ is not too close to the epidemic threshold, as shown in Fig. 3. As previously reported in the continuous case [13,17], the mean-field scaling

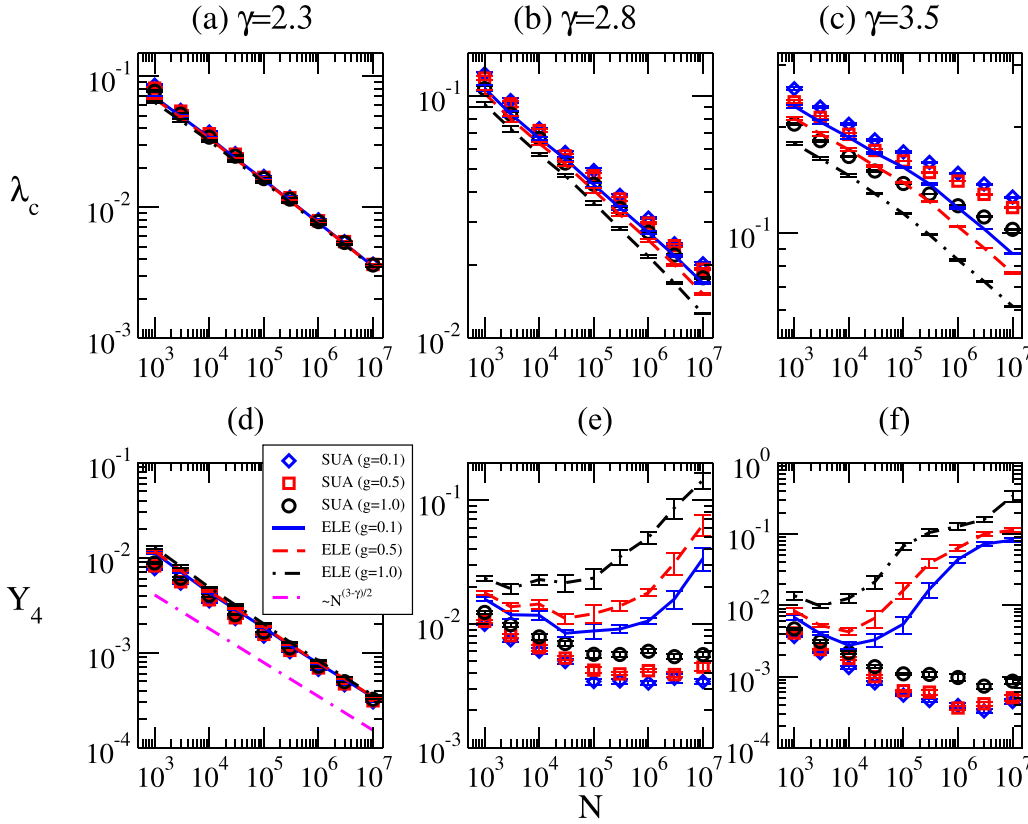


FIG. 2. Finite-size analysis of epidemic threshold (top) and IPR (bottom) for ELE and discrete-time simulations (SUA). Power-law networks with degree exponents (a), (d) $\gamma = 2.3$, (b), (e) $\gamma = 2.8$, and (c), (f) $\gamma = 3.5$ and three values of $g = 0.1, 0.5$, and 1 are presented. The magenta dashed line represents $Y_4 \sim N^{-(3-\gamma)/2}$. We adopted $k_c = 2\sqrt{N}$ and $k_c \sim N^{1/\gamma}$ for $\gamma < 3$ and $\gamma > 3$, respectively.

with $\theta = 1$ is confirmed if one is not too close to the epidemic threshold. The scaling $\theta = 1$ remains valid for $g \in [0.1, 1]$, while deviations are expected for $g \ll 1$ where the continuous-time limit occurs. The deviation of the linear scal-

ing observed for finite g (finite Δt) shrinks as the network size increases indicating that it is a finite-size effect due to falling onto the absorbing state. Here, a crucial difference between discrete- and continuous-time analyses is observed: the scaling region with exponent $\theta = 1/(3 - \gamma)$, rigorously obtained in a continuous-time version [38] and reproduced in extensive numerical continuous simulations [13], is not observed in the discrete-time simulations discussed in Fig. 3. In principle, both continuous- or discrete-time approaches are dealing with the same phenomena: epidemic processes with recurrent infections, no immunity, on the top of power-law networks. Universality states that no relevant differences are expected once overall aspects, such as symmetries and underlying structure, are preserved. So, it is surprising that the approaches sharing essentially the same properties, except the discrete nature of the time, lead to a contrasting critical exponent. This result represents an important issue when choosing the theoretical approach to model epidemic spreading on networks. Considering the regime of high prevalence, we observe that MMCA and ELE present a dependence with g and there is a convergence to their respective theoretical continuous limit prevalence when $g \rightarrow 0$, as shown in Figs. 4(a) and 4(b), respectively. Such as in the continuous-time limit, the introduction of dynamical correlation leads to an almost perfect match between ELE and SUA simulations. For not too high prevalence, ELE theory performs better for smaller time steps, reaching the maximum performance in the continuous-time limit as shown in the inset of Fig. 4(b). Interestingly, the

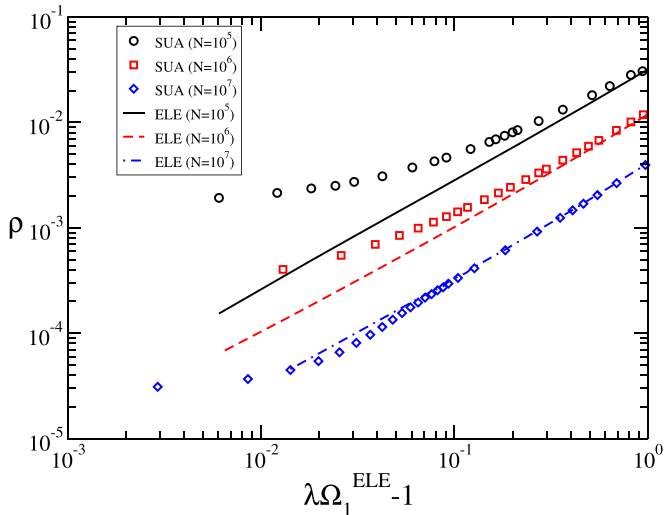


FIG. 3. Comparison of epidemic prevalence for SUA simulations (symbols) and ELE (dashed lines) mean-field theory with $g = \mu \Delta t = 0.5$. We consider power-law networks with degree exponent $\gamma = 2.3$ and sizes $N = 10^5, 10^6$, and 10^7 . We adopted $k_c = 2\sqrt{N}$.

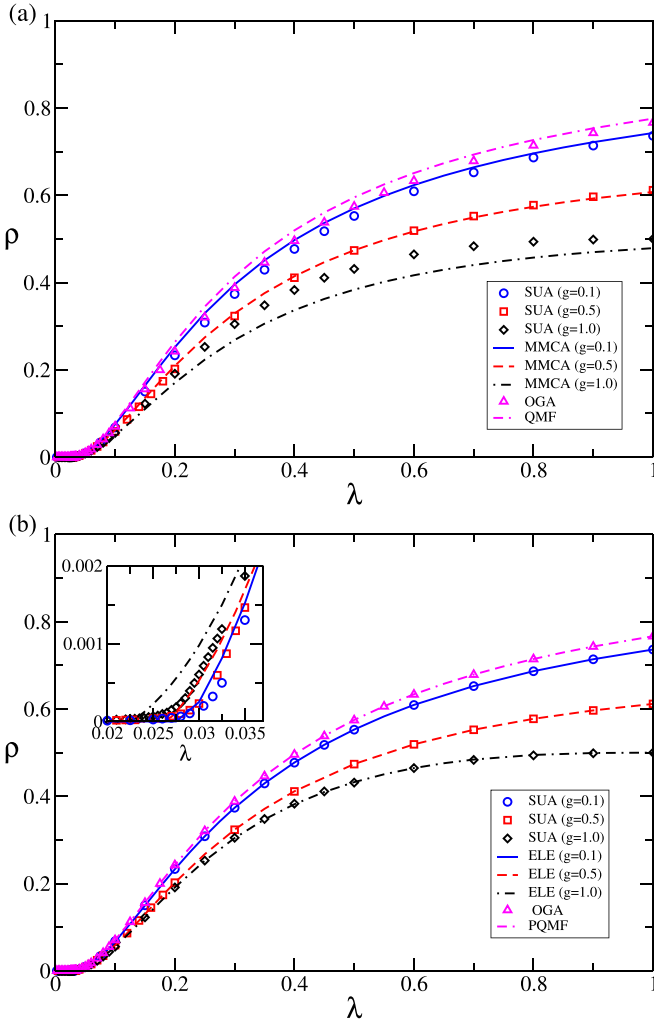


FIG. 4. Prevalence as a function of the ratio $\lambda = \beta/\mu$ for discrete-time theory and simulations considering $\mu = 1.0$ and the uncorrelated power-law degree distribution network with $\gamma = 2.8$. We adopted $N = 10^6$ and $k_c = 2\sqrt{N}$. The choice of μ limits the allowed values of $g = \mu\Delta t$. Both (a) MMCA and (b) ELE theories are presented. Inset shows a zoom in the low prevalence regime. Continuous-time limits of both theories (QMF and PQMF, respectively) are shown for sake of comparison.

discrete-time theories approach the continuous limit ($g \rightarrow 0$) from below in the regime of high prevalence [Fig. 4(b), main plot] while, near to the critical point, it converges from above [Fig. 4(b), inset].

IV. CONCLUSIONS

The art of modeling epidemic processes on networks has been improved continuously with the implementation of elaborated aspects of the dynamical rules such as the precise role of absorbing states [43,50], localization phenomena [16,32],

and non-Markovian nature [51–53]. Mean-field approaches are primordial allies in the understanding of epidemic processes on networks and their accuracy must be probed using extensive and statistically exact stochastic simulations [12,43,48]. Computer simulations are implemented using discrete time: the continuous version considers asynchronous updates with variable time steps, while the discrete one is performed with synchronous updates with fixed time steps. So, despite continuous-time approaches seeming more natural for actual epidemic processes, discrete-time versions are very popular [19,22,31] due to their easier computer implementation and also their flexibility to build models with more complex aspects in a simpler way in terms of probabilities instead of rates. However, epidemic processes on networks can be puzzling [36,54] and dependent on the slightly different model details [55]. Therefore, the role of synchronous and asynchronous approaches is worthy of investigation.

In the present work, we scrutinized the effects of discrete- and continuous-time versions of the SIS epidemic model considering stochastic simulations as well as one-node and pairwise mean-field theories. Analyzing the epidemic threshold and the localization of the epidemic prevalence near the transition, we report that discrete-time approaches are dependent on the time-step size, while differences between discrete and continuous cases disappear as the time step goes to zero. While the previous findings are not surprising, we report a crucial difference between continuous- and discrete-time simulations: the epidemic prevalence near the epidemic threshold goes to zero following different scaling exponents $\rho \sim (\lambda - \lambda_c)^\theta$, where the former is given by the exact exponent $\theta = 1/(3 - \gamma)$ reported by Chatterjee and Durrett [39], while the latter still provide the mean-field exponent $\theta = 1$ [13,16,22]. While determining which approach describes a better real-world spreading process is beyond the scope of the present work, our results raise important concerns on the choice of the theoretical and simulation approaches that can be present in other epidemic models or, more generally, dynamical processes on complex networks rather than the SIS model investigated in the present work.

ACKNOWLEDGMENTS

D.H.S. acknowledges the support given by Fundação de Amparo à Pesquisa do Estado de São Paulo (FAPESP), Brazil (Grants No. 2021/00369-0 and No. 2013/07375-0). F.A.R. acknowledges Conselho Nacional de Desenvolvimento Científico e Tecnológico (CNPq), Brazil (Grant No. 308162/2023-4) and FAPESP (Grant No. 19/23293-0) for the financial support given for this research. This research was conducted with the computational resources of the Center for Research in Mathematical Sciences Applied to Industry (CeMEAI) funded by FAPESP (Grant No. 2013/07375-0). S.C.F. acknowledges the support by the CNPq (Grant No. 310984/2023-8).

[1] R. Pastor-Satorras, C. Castellano, P. Van Mieghem, and A. Vespignani, Epidemic processes in complex networks, *Rev. Mod. Phys.* **87**, 925 (2015).

[2] G. F. de Arruda, F. A. Rodrigues, and Y. Moreno, Fundamentals of spreading processes in single and multilayer complex networks, *Phys. Rep.* **756**, 1 (2018).

- [3] W. Wang, M. Tang, H. E. Stanley, and L. A. Braunstein, Unification of theoretical approaches for epidemic spreading on complex networks, *Rep. Prog. Phys.* **80**, 036603 (2017).
- [4] A. N. Desai, M. U. G. Kraemer, S. Bhatia, A. Cori, P. Nouvellet, M. Herringer, E. L. Cohn, M. Carrion, J. S. Brownstein, L. C. Madoff, and B. Lassmann, Real-time epidemic forecasting: Challenges and opportunities, *Health Security* **17**, 268 (2019).
- [5] A. G. Muñoz, M. C. Thomson, A. M. Stewart-Ibarra, G. A. Vecchi, X. Chourio, P. Nájera, Z. Moran, and X. Yang, Could the recent zika epidemic have been predicted? *Front. Microbiol.* **8**, 1291 (2017).
- [6] M. F. C. Gomes, A. P. Piontti, L. Rossi, D. L. Chao, I. Longini, M. E. Halloran, and A. Vespignani, Assessing the international spreading risk associated with the 2014 West African Ebola outbreak, *PLoS Curr.* **6** (2014).
- [7] A. Arenas, W. Cota, J. Gómez-Gardeñes, S. Gómez, C. Granell, J. T. Matamalas, D. Soriano-Paños, and B. Steinegger, Modeling the spatiotemporal epidemic spreading of COVID-9 and the impact of mobility and social distancing interventions, *Phys. Rev. X* **10**, 041055 (2020).
- [8] G. S. Costa, W. Cota, and S. C. Ferreira, Outbreak diversity in epidemic waves propagating through distinct geographical scales, *Phys. Rev. Res.* **2**, 043306 (2020).
- [9] M. J. Keeling and P. Rohani, *Modeling Infectious Diseases in Humans and Animals* (Princeton University Press, Princeton, NJ, 2011), pp. 1–368.
- [10] A. Barrat, M. Barthélemy, and A. Vespignani, *Dynamical Processes on Complex Networks* (Cambridge University Press, Cambridge, UK, 2008).
- [11] M. Newman, *Networks: An Introduction* (Oxford University Press, Inc., New York, 2010).
- [12] A. S. Mata and S. C. Ferreira, Pair quenched mean-field theory for the susceptible-infected-susceptible model on complex networks, *Europhys. Lett.* **103**, 48003 (2013).
- [13] D. H. Silva, S. C. Ferreira, W. Cota, R. Pastor-Satorras, and C. Castellano, Spectral properties and the accuracy of mean-field approaches for epidemics on correlated power-law networks, *Phys. Rev. Res.* **1**, 033024 (2019).
- [14] P. Van Mieghem, The viral conductance of a network, *Computer Commun.* **35**, 1494 (2012).
- [15] P. Van Mieghem, Epidemic phase transition of the SIS type in networks, *Europhys. Lett.* **97**, 48004 (2012).
- [16] A. V. Goltsev, S. N. Dorogovtsev, J. G. Oliveira, and J. F. F. Mendes, Localization and spreading of diseases in complex networks, *Phys. Rev. Lett.* **109**, 128702 (2012).
- [17] D. H. Silva, F. A. Rodrigues, and S. C. Ferreira, High prevalence regimes in the pair-quenched mean-field theory for the susceptible-infected-susceptible model on networks, *Phys. Rev. E* **102**, 012313 (2020).
- [18] L. Li, G.-Q. Sun, and Z. Jin, Bifurcation and chaos in an epidemic model with nonlinear incidence rates, *Appl. Math. Comput.* **216**, 1226 (2010).
- [19] S. Gómez, A. Arenas, J. Borge-Holthoefer, S. Meloni, and Y. Moreno, Discrete-time Markov chain approach to contact-based disease spreading in complex networks, *Europhys. Lett.* **89**, 38009 (2010).
- [20] S. Gómez, J. Gómez-Gardeñes, Y. Moreno, and A. Arenas, Nonperturbative heterogeneous mean-field approach to epidemic spreading in complex networks, *Phys. Rev. E* **84**, 036105 (2011).
- [21] C. Granell, S. Gómez, and A. Arenas, Dynamical interplay between awareness and epidemic spreading in multiplex networks, *Phys. Rev. Lett.* **111**, 128701 (2013).
- [22] J. T. Matamalas, A. Arenas, and S. Gómez, Effective approach to epidemic containment using link equations in complex networks, *Sci. Adv.* **4**, eaau4212 (2018).
- [23] H. J. Ahn and B. Hassibi, Global dynamics of epidemic spread over complex networks, in *52nd IEEE Conference on Decision and Control* (IEEE, New York, 2013), pp. 4579–4585.
- [24] X. Wang, Z. Wang, and H. Shen, Dynamical analysis of a discrete-time sis epidemic model on complex networks, *Appl. Math. Lett.* **94**, 292 (2019).
- [25] Y. Wang, D. Chakrabarti, C. Wang, and C. Faloutsos, Epidemic spreading in real networks: An eigenvalue viewpoint, in *22nd International Symposium on Reliable Distributed Systems, 2003, Proceedings* (Florence, Italy, 2003), pp. 25–34.
- [26] D. Chakrabarti, Y. Wang, C. Wang, J. Leskovec, and C. Faloutsos, Epidemic thresholds in real networks, *ACM Trans. Inf. Syst. Secur.* **10**, 1 (2008).
- [27] P. C. V. da Silva, F. Velásquez-Rojas, C. Connaughton, F. Vazquez, Y. Moreno, and F. A. Rodrigues, Epidemic spreading with awareness and different timescales in multiplex networks, *Phys. Rev. E* **100**, 032313 (2019).
- [28] X. Wang, X. Zhu, X. Tao, J. Xiao, W. Wang, and Y.-C. Lai, Anomalous role of information diffusion in epidemic spreading, *Phys. Rev. Res.* **3**, 013157 (2021).
- [29] J. Gómez-Gardeñes, D. Soriano-Paños, and A. Arenas, Critical regimes driven by recurrent mobility patterns of reaction-diffusion processes in networks, *Nat. Phys.* **14**, 391 (2018).
- [30] W. Cota, D. Soriano-Paños, A. Arenas, S. C. Ferreira, and J. Gómez-Gardeñes, Infectious disease dynamics in metapopulations with heterogeneous transmission and recurrent mobility, *New J. Phys.* **23**, 073019 (2021).
- [31] D. Soriano-Paños, W. Cota, S. C. Ferreira, G. Ghoshal, A. Arenas, and J. Gómez-Gardeñes, Modeling communicable diseases, human mobility, and epidemics: A review, *Ann. Phys. (Leipzig)* **534**, 2100482 (2022).
- [32] D. H. Silva and S. C. Ferreira, Dissecting localization phenomena of dynamical processes on networks, *J. Phys.: Complexity* **2**, 025011 (2021).
- [33] R. Pastor-Satorras and C. Castellano, Eigenvector localization in real networks and its implications for epidemic spreading, *J. Stat. Phys.* **173**, 1110 (2018).
- [34] J. C. M. Silva, D. H. Silva, F. A. Rodrigues, and S. C. Ferreira, Comparison of theoretical approaches for epidemic processes with waning immunity in complex networks, *Phys. Rev. E* **106**, 034317 (2022).
- [35] R. Pastor-Satorras and C. Castellano, Distinct types of eigenvector localization in networks, *Sci. Rep.* **6**, 18847 (2016).
- [36] C. Castellano and R. Pastor-Satorras, Competing activation mechanisms in epidemics on networks, *Sci. Rep.* **2**, 371 (2012).
- [37] S. N. Dorogovtsev, A. V. Goltsev, and J. F. F. Mendes, k -core organization of complex networks, *Phys. Rev. Lett.* **96**, 040601 (2006).
- [38] T. Mountford, D. Valesin, and Q. Yao, Metastable densities for the contact process on power law random graphs, *Electron. J. Probab.* **18**, 36 (2013).
- [39] S. Chatterjee and R. Durrett, Contact processes on random graphs with power law degree distributions have critical value 0, *Ann. Probab.* **37**, 2332 (2009).

- [40] P. G. Fennell, S. Melnik, and J. P. Gleeson, Limitations of discrete-time approaches to continuous-time contagion dynamics, *Phys. Rev. E* **94**, 052125 (2016).
- [41] X. Chang and C.-R. Cai, Analytical computation of the epidemic prevalence and threshold for the discrete-time susceptible-infected-susceptible dynamics on static networks, *Physica A* **571**, 125850 (2021).
- [42] L. Zhang, C.-R. Cai, J.-Q. Zhang, X.-S. Liu, C.-Y. Wang, and Z.-X. Wu, Nonlinear mapping between continuous- and discrete-time dynamics, *Europhys. Lett.* **137**, 61002 (2022).
- [43] W. Cota and S. C. Ferreira, Optimized gillespie algorithms for the simulation of Markovian epidemic processes on large and heterogeneous networks, *Comput. Phys. Commun.* **219**, 303 (2017).
- [44] S. Gómez, A. Arenas, J. Borge-Holthoefer, S. Meloni, and Y. Moreno, Probabilistic framework for epidemic spreading in complex networks, *Int. J. Complex Syst. Sci.* **1**, 47 (2011).
- [45] C.-R. Cai, Z.-X. Wu, and J.-Y. Guan, Effective degree Markov-chain approach for discrete-time epidemic processes on uncorrelated networks, *Phys. Rev. E* **90**, 052803 (2014).
- [46] M. M. de Oliveira and R. Dickman, How to simulate the quasistationary state, *Phys. Rev. E* **71**, 016129 (2005).
- [47] R. S. Sander, G. S. Costa, and S. C. Ferreira, Sampling methods for the quasistationary regime of epidemic processes on regular and complex networks, *Phys. Rev. E* **94**, 042308 (2016).
- [48] S. C. Ferreira, C. Castellano, and R. Pastor-Satorras, Epidemic thresholds of the susceptible-infected-susceptible model on networks: A comparison of numerical and theoretical results, *Phys. Rev. E* **86**, 041125 (2012).
- [49] M. Catanzaro, M. Boguñá, and R. Pastor-Satorras, Generation of uncorrelated random scale-free networks, *Phys. Rev. E* **71**, 027103 (2005).
- [50] G. S. Costa and S. C. Ferreira, Simple quasistationary method for simulations of epidemic processes with localized states, *Comput. Phys. Commun.* **267**, 108046 (2021).
- [51] M. Feng, S.-M. Cai, M. Tang, and Y.-C. Lai, Equivalence and its invalidation between non-Markovian and Markovian spreading dynamics on complex networks, *Nat. Commun.* **10**, 3748 (2019).
- [52] M. Boguñá, L. F. Lafuerza, R. Toral, and M. A. Serrano, Simulating non-Markovian stochastic processes, *Phys. Rev. E* **90**, 042108 (2014).
- [53] P. Van Mieghem and R. van de Bovenkamp, Non-Markovian infection spread dramatically alters the susceptible-infected-susceptible epidemic threshold in networks, *Phys. Rev. Lett.* **110**, 108701 (2013).
- [54] A. S. Mata and S. C. Ferreira, Multiple transitions of the susceptible-infected-susceptible epidemic model on complex networks, *Phys. Rev. E* **91**, 012816 (2015).
- [55] W. Cota, A. S. Mata, and S. C. Ferreira, Robustness and fragility of the susceptible-infected-susceptible epidemic models on complex networks, *Phys. Rev. E* **98**, 012310 (2018).